Electric Dipole (Hyper)polarizabilities of Selected X2Y2 and X3Y3 (X = Al, Ga, In and Y = P, As): III−V Semiconductor Clusters. An ab Initio Comparative Study

3 AUTHORS, INCLUDING:

Panaghiotis Karamanis
French National Centre for Scientific Resea…
55 PUBLICATIONS **679** CITATIONS

SEE PROFILE

Claude Pouchan
Université de Pau et des Pays de l'Adour
192 PUBLICATIONS **2,577** CITATIONS

SEE PROFILE

Electric Dipole (Hyper)polarizabilities of Selected X_2Y_2 and X_3Y_3 (X = Al, Ga, In and Y = P, As): III−V Semiconductor Clusters. An ab Initio Comparative Study

Panaghiotis Karamanis,*,†,‡ Claude Pouchan,§ and Jerzy Leszczynski⊥,‡

Department of Chemistry, Jackson State University, 1400 J. R. Lynch Street, P.O. Box 17910, Jackson, Mississippi 39217, and Groupe de Chimie Théorique et Réactivité, ECP, IPREM UMR 5254, Université de Pau et de Pays de l'Adour, 64075 Pau Cedex, France

A systematic ab initio comparative study of the (hyper)polarizabilities of selected III−V stoichiometric semiconductor clusters has been carried out. Our investigation focuses on the ground state structures of the dimers and on two dissimilar trimer configurations of aluminum, gallium, indium phosphide and arsenide. The basis set effect on both the polarizabilities and hyperpolarizabilities of the studied systems has been explicitly taken into account relying on the augmented correlation consistent aug-cc-pVnZ (n = D, T, Q, and 5) basis sets series. In addition, a rough estimation of the effects of the relativistic effects on the investigated properties is provided by extension of the study to include calculations performed with relativistic electron core potentials (or pseudopotentials). Electron correlation effects have been estimated utilizing methods of increasing predictive reliability, e.g., the Møller−Plesset many body perturbation theory and the couple cluster approach. Our results reveal that in the considered semiconductor species the Group III elements (Al, Ga, In) play a vital role on the values of their relative (hyper)polarizability. At all levels of theory employed the most hyperpolarizable clusters are the indium derivatives while the aluminum arsenide clusters also exhibit high, comparable hyperpolarizabilities. The less hyperpolarizable species are those composed of gallium and this is associated with the strong influence of the nuclear charge on the valence electrons of Ga due to the poor shielding that is provided by the semicore d electrons. In addition, the analysis of the electronic structure and the hyperpolarizability magnitudes reveals that clusters, in which their bonding is characterized by strong electron transfer from the electropositive to the electronegative atoms, are less hyperpolarizable than species in which the corresponding electron transfer is weaker. Lastly, from the methodological point of view our results point out that the hyperpolarizabilities of those species converge when an augmented triple-ζ quality basis set is used and, also, that the second order Møller−Plesset approximation (MP2) overestimates considerably their second hyperpolarizabilities with respect to the highest level of coupled cluster theory applied in this study (CCSD(T)).

Introduction

The desire to understand the undergoing transformation in the properties of materials as their size increases and wide range of technological applications of semiconductors due to their unique electronic properties has triggered an explosion of theoretical and experimental studies. The investigations include clusters and low-dimensional fragments of a vast assortment of semiconductor materials.[1,2] Consequently, a substantial fraction of the reported experimental[3−10] and theoretical[11−21] studies has been devoted to their electronic properties. Among them are the following: ionization potentials electron affinities, their spectroscopic properties including the photoelectron spectra, or properties related to the response of those species to the interaction with light or an external electric field such as their optical absorption, or their linear and nonlinear optical properties. Especially, their nonlinear optical properties[22−24] are considered of great technological merit since it is believed that low-dimensional semiconductor materials may offer a new ground in the development and design of novel cluster based NLO materials.

The last perspective has motivated a considerable number of attempts to study and predict the microscopic linear and nonlinear optical properties, as they reflect on their molecular (hyper)polarizabilities.[25−32] Not surprisingly, a significant amount of the previous cluster studies focus on the size effect on those microscopic properties since the size of the cluster plays a vital role on their response to the external electric field. However, there is another factor that should also be taken into account, and this is the cluster composition. In this area, only two systematic studies have investigated both factors within the TDHF framework. The first study was published by Korabath and Karna et al.,[30] who investigated the dipole polarizabilities and first hyperpolarizabilities of Ga_nN_n, Ga_nP_n, and Ga_nAs_n clusters within the TDHF framework, and the second by Lan et al.,[31] who explored the first hyperpolarizabilities of Ga_3As_3, Ga_3Sb_3, In_3P_3, In_3As_3, and In_3Sb_3.

In this work we report a systematic ab initio comparative study of the dipole polarizabilities and the second hyperpolarizabilities of clusters composed by selected III−V elements. These species have attracted considerable attention due to their interesting structural, optical, and spectroscopic properties.[3−31] Our aim is to provide an accurate picture of how these properties

* Corresponding author.
† E-mail: pkar@ccmsi.us; panos@chemistry.upatras.gr.
‡ Jackson State University. E-mail: claude.pouchan@univ-pau.fr.
§ Université de Pau et de Pays de l'Adour.
⊥ E-mail: jerzy@ccmsi.us.

Electric Dipole (Hyper)polarizabilities

J. Phys. Chem. A, Vol. 112, No. 51, 2008 **13663**

evolve when one component of a given cluster is changed. The considered clusters are composed of Al, Ga, and In elements combined with P and As in a stoichiometric fashion. All of these systems have been the subjects of previous experimental[3–10] and theoretical studies[11–20,25–31] with respect to their structural, electronic, and spectroscopic properties. Although there are (hyper)polarizability values available for a few of those species,[25,28] no systematic study on their linear and nonlinear microscopic polarizabilities has been reported for the entire series.

Our investigation started by exploring the ground state structures of the Al_2P_2, Al_2As_2, Ga_2P_2, Ga_2As_2, In_2P_2, and In_2As_2 dimers. For all the dimers, the lowest energy configurations are represented by a rhomboidal shape of D_{2h} symmetry ($^1A_{1g}$)[11–17] where the electropositive atoms (Al, Ga, In) are located on the long diagonal and the electronegative atoms (P, As) on the short one. The small size of these systems allows us to study explicitly basis set and electron correlation contributions that are expected to play a central role on the reliable prediction of their microscopic (hyper)polarizabilities. In addition, their similar geometric configurations and common bonding characteristics are expected to make the comparison between their (hyper)polazibilities a quite straightforward task. Next, we extended the comparative study to the trimers of these species. For the trimers the ground state configurations vary as we move down the periodic table. For instance, the ground state structure of Al_3P_3 according to most of the previous studies[18,28] adopts a planar configuration of D_{3h} symmetry characterized by alternating Al–P bonding. The same holds for the ground state structure of Al_3As_3.[17] In striking contrast, the established ground state structures of Ga_3As_3[17,25] and In_3As_3[16] are represented by three-dimensional configurations of C_s symmetry. It has been shown[27,28] that the microscopic features such as the cluster's shape and bonding may affect dramatically the (hyper)polarizabilities of a given cluster; hence, any rational comparison between the (hyper)polarizabilities of clusters composed by different elements should definitely involve species which possess similar structural and bonding patterns. Thus, to obtain a global picture that will include also possible bonding and structural effects on the properties of interest, we considered in our study both of the trimer isomers which are competing for the X_3Y_3 ground states since they are characterized by totally dissimilar bonding and shapes.

Theory Applied and Computational Details

The electronic dipole (hyper)polarizabilities, in their static form, can be defined by the Taylor series expansion[33] of the perturbed energy of an atom (or molecule) in the presence of a weak uniform external static electric field:

$$E^p = E^0 - \mu_\alpha F_\alpha - \frac{1}{2}\alpha_{\alpha\beta}F_aF_\beta - \frac{1}{6}\beta_{\alpha\beta\gamma}F_\alpha F_\beta F_\gamma -$$
$$\frac{1}{24}\gamma_{\alpha\beta\gamma\delta}F_\alpha F_\beta F_\gamma F_\delta + \dots \quad (1)$$

E^p is the energy of the atomic (or molecular) system in the presence of the static electric field (F), E^0 is its energy in the absence of the field, μ_α corresponds to the permanent dipole moment of the system, $\alpha_{\alpha\beta}$ is the static dipole polarizability tensor, and $\beta_{\alpha\beta\gamma}$ and $\gamma_{\alpha\beta\gamma\delta}$ are the first and second dipole hyperpolarizabilities, respectively. Greek subscripts denote tensor components and can be equal to x, y, and z and each repeated subscript implies summation over x, y, and z.

The components of each tensor of eq 1 can be computed by applying carefully chosen static weak electric fields relying on the finite field technique (FF).[34] Since in the version of the FF technique we use here[35] the key quantity is the field-dependent energy of the cluster, the obtained solutions are consistent regardless if the methods we consider satisfy or not the Hellmann–Feynman theorem (such as the Hartree–Fock (HF) and the Møller–Plesset (MP) many body perturbation theory respectively). Once the Cartesian components of each tensor are obtained the mean (or average) static dipole polarizability ($\bar{\alpha}$), the anisotropy ($\Delta\alpha$) of the polarizability tensor, and the scalar component of the second hyperpolarizability tensor $\bar{\gamma}$ can be computed. Those quantities are related to the experiment and in terms of the Cartesian components are defined as:

$$\bar{\alpha} = \frac{1}{3}(\alpha_{xx} + \alpha_{yy} + \alpha_{zz}) \quad (2)$$

$$\Delta\alpha = \left(\frac{1}{2}\right)^{1/2}[(\alpha_{xx} - \alpha_{yy})^2 + (\alpha_{xx} - \alpha_{zz})^2 + (\alpha_{zz} - \alpha_{yy})^2 +$$
$$6(\alpha_{xy}^2 + \alpha_{xz}^2 + \alpha_{zy}^2)]^{1/2} \quad (3)$$

$$\bar{\gamma} = \frac{1}{5}(\gamma_{xxxx} + \gamma_{yyyy} + \gamma_{zzzz}) + \frac{2}{5}(\gamma_{xxyy} + \gamma_{yyzz} + \gamma_{xxzz}) \quad (4)$$

The simplest level of theory that uses the FF technique in this work is the Hartree–Fock approximation where the field-induced relaxation of the orbitals is taken into account through the self-consistent field (SCF). Then electron correlation[36–38] is included via the framework of the Møller–Plesset many body perturbation theory and its various orders such as the second order MP (MP2) and the fourth order MP including single, double, triple, and quadruple substitutions (MP4(SDTQ) hereafter MP4), singles and doubles coupled-cluster (CCSD), and at the highest level CCSD(T), which includes an estimate of connected triple excitations via a perturbational treatment. All the aforementioned calculations were carried out with the GAUSSIAN 98 suite of programs.[39]

One of the central elements in the computation of reliable (hyper)polarizability values is the basis set choice. In the present work which involves a comparative study of systems consisting of different elements this issue becomes more important and somewhat more complex since basis sets of similar type should be considered in order to obtain a reliable estimation of the relative magnitudes of these properties over all the cluster species. In addition, in systems built up from heavy elements one should use relativistic pseudopotential basis sets (PP) to obtain an estimation of the magnitude of those effects on the properties of interest. What is more, for systems where light and heavy elements coexist, the utilization of mixed basis sets consisting of all electron basis sets for the light atoms and relativistic pseudopotential basis sets (PP) for the heavy ones cannot be avoided. This may cause considerable problems in the evaluation of the possible (hyper)polarizability differences, since it may not be clear whether they are a subject of the different linear or nonlinear response of each cluster to the electric field or, simply, are caused by the various types of basis sets (all electron or PP) used for each molecule. For this reason, we performed a careful basis set study to test the performance, especially of mixed basis sets in the calculation of the dipole polarizabilities and the second dipole hyperpolarizabilities of those species.

The basis sets we used are of the all electron type (all electrons of an atom are explicitly described by Gaussian basis functions) and of the small core pseudopotential (PP) or electron core potential type (a small number of core electrons are approximated by a relativistic effective potential). Though the small core PPs are more computationally expensive, nevertheless
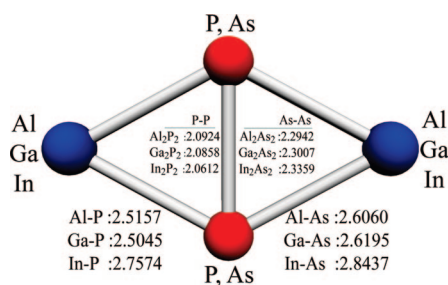
13664 *J. Phys. Chem. A, Vol. 112, No. 51, 2008*

Karamanis et al.

Figure 1. MP2/cc-pVTZ optimized bond lengths of M_2X_2 clusters (M = Al, Ga In, X = P, As).

they do not suffer from overestimations of valence electron correlation energies[40] and/or insufficient Pauli repulsion between valence and core electrons,[41] which are expected to affect valence properties such as the (hyper)polarizabilities.

Following the above rationale, for Al_2P_2, we used only the aug-cc-pVDZ,[42] aug-cc-pVTZ,[43] and aug-cc-pVQZ[43] all electron basis sets. In the cases of Al_2As_2, Ga_2P_2, and In_2P_2 we assessed the performance of the following mixed basis set series: Al_2As_2—all electron aug-cc-pVDZ(D,T,Q)Z for Al and small core pseudopotential aug-cc-pV(D,T,Q)Z-PP for As; Ga_2P_2—all electron aug-cc-pVDZ(D,T,Q)Z for P and small core pseudopotential aug-cc-pV(D,T,Q)Z-PP for Ga; In_2P_2—all electron aug-cc-pVDZ(D,T,Q)Z for P and small core pseudopotential aug-cc-pV(D,T,Q)Z-PP for In. Lastly, for In_2As_2 we used only relativistic small core pseudopotential basis sets. It is important to note that the augmented PPs have been used previously in (hyper)polarizability computations on different atomic and molecular systems. For instance, Jansik et al.[45] and Cundari et al.[46] showed that ECPs provide similar results as the all electron basis sets as long as comparable valence basis sets are used. Finally, it should be noted that all (hyper)polarizability values discussed in this work are in atomic units.

Results and Discussion

Figure 1 illustrates the optimized geometries of the dimer ground states at the MP2/cc-pVTZ level of theory. Table 1 lists the SCF values of the mean polarizabilities, the polarizability anisotropies, and the mean second hyperpolarizabilities of all dimers predicted by using the basis set of double, triple, and quadruple ζ quality. It should be stressed that the reliability of the FF approach used in this work has been tested for Al_2P_2 at the HF level. The obtained mean (hyper)polarizabilities for this cluster obtained from our FF approach are as follows: $\bar{\alpha}_{\text{aug-ccp-VDZ}} \equiv 148.24$ and $\bar{\alpha}_{\text{aug-ccp-VTZ}} \equiv 148.40$, $\bar{\gamma}_{\text{aug-ccp-VDZ}} \equiv 132 \times 10^3$, and $\bar{\gamma}_{\text{aug-ccp-VTZ}}$ 144×10^3. These values are in very good agreement with analytic calculations[47] which yield $\bar{\alpha}_{\text{aug-ccp-VDZ}} \equiv 148.243$, $\bar{\alpha}_{\text{aug-ccp-VTZ}} \equiv 148.397$, $\bar{\gamma}_{\text{aug-ccp-VDZ}} \equiv 132.68 \times 10^3$, and $\bar{\gamma}_{\text{aug-ccp-VDZ}} \equiv 143.68 \times 10^3$.

For the AlP dimer our best polarizability and polarizability anisotropy HF level values, predicted with the aug-cc-pVQZ basis set, amount to 148.54 and 102.30, respectively. These values are in good agreement with our previous SCF calculation[29] with the 6-31+G(3df) basis set at the B3LYP/6-31+G(d) equilibrium geometry, which yielded values of 151.05 and 107.47 $e^2 \alpha_0^2 E_h^{-1}$ for the mean polarizability and the polarizability anisotropy, respectively. As has been mentioned in that paper, geometry optimizations at the MP2 level of theory yield slightly more compact cluster structures than those obtained by using the B3LYP functional and this reflects on the magnitude of their polarizability. The effect of the cluster geometry on the polarizability values is more pronounced in the case of the

GaAs dimer. In this case a previously reported polarizability value[25] obtained with the aug-cc-pVTZ-PP basis set at the B3LYP optimized geometries amounts to 159.91 $e^2 \alpha_0^2 E_h^{-1}$, which is about 4.5 $e^2 \alpha_0^2 E_h^{-1}$ larger than in the present case (155.42 $e^2 \alpha_0^2 E_h^{-1}$).

Basis Set Effect. The effect of the basis set enhancement on the (hyper)polarizabilities of the cluster dimers is similar to the trend that has been observed in previous studies on Al_2P_2[28,29] and Ga_2As_2[26] clusters. The best polarizability and polarizability anisotropy values which were predicted with the aug-cc-pVQZ basis sets (all electron or PP) are in very close proximity (<1% differences) to those obtained with the smallest aug-cc-pVDZ basis set. However, this is not the case for the second hyperpolarizability which, in principle, depends considerably on the higher angular momentum basis functions. Overall, for all the dimers the increase of the basis set size leads to higher values for both the mean polarizability and the second hyperpolarizability. As expected, the largest improvement of the hyperpolarizability values is observed for the transition from the aug-cc-pVDZ to aug-cc-pVTZ basis set while the use of the very large aug-cc-pVQZ set changes less considerably the (hyper)polarizability values compared to those obtained with the aug-cc-pVTZ set. Table 2 presents the convergence of all the hyperpolarizability components of Al_2P_2 and Ga_2As_2 with respect to the basis set used at the HF level. As expected the additional diffuse d and especially the f Gaussian type functions (GTF) that are included in the triple-ζ basis set affect mostly the γ_{xxxx} (perpendicular to the cluster plan), γ_{yyyy} (perpendicular to the P—P and As—As bonds), and γ_{xxyy} components. On the other hand γ_{zzzz}, which is expected to be sensitive to the diffuse s- and p-GTF, converge fast with the basis set size. For both γ_{xxxx} and γ_{xxyy} the aug-cc-pVTZ set yields about 23% larger values than aug-cc-pVDZ while the improvement for γ_{zzzz} is only 3%. Interestingly the g GTFs of aug-cc-pVQZ seems to be important for γ_{xxxx}, γ_{xxyy}, and γ_{yyyy} since the obtained values with this basis set component are about 9%, 8%, and 6% larger than those calculated with the aug-cc-pVTZ basis set. Nevertheless, the effect of the g functions does not reflect considerably on the mean hyperpolarizability since the latter quantity is dominated by the γ_{zzzz} component, which is not affected by GTFs of that type. In addition, for both Al_2P_2 and Ga_2As_2 we used the aug-cc-pV5Z basis set in order to check the contribution of the h GTFs on the hyperpolarizabilities of those systems. As is seen in Table 2 no significant improvement is observed at the HF level. Concerning the performance of the PP basis sets compared to their all electron versions our results show that, at the HF level, these two basis set classes operate in a quiet similar manner. For Al_2As_2 the predicted polarizability values using the all electron basis sets are very close to the ones calculated with the basis set constructed by an all electron set for Al and a PP set for the electronegative As. The obtained mean polarizabilities with the latter basis sets are about 0.5% larger than the ones predicted with their all electron counterparts. The opposite trend is revealed in the cases of Ga_2P_2 and Ga_2As_2. For these clusters the PP basis sets yield about 1.1–1.7% smaller polarizabilities than the corresponding all electron set values. The same trend is observed for the second hyperpolarizabilities; however, in this case the differences are larger than what has been observed for the dipole polarizabilities. For instance, the largest PP basis sets predict 2% larger hyperpolarizabilities for Al_2As_2 and about 4–5% smaller mean hyperpolarizabilities for Ga_2P_2 and Ga_2As_2. In all these cases the differences are so small that it is not easy to identify with absolute certainty whether they are caused by the different description of the valence

Electric Dipole (Hyper)polarizabilities

J. Phys. Chem. A, Vol. 112, No. 51, 2008 **13665**

TABLE 1: Basis Set Dependence of the Mean Dipole Polarizability ($\bar{\alpha}/e^2\ a_0^2\ E_h^{-1}$), the Polarizability Anisotropy ($\Delta\alpha/e^2\ a_0^2\ E_h^{-1}$), and the Mean Dipole Hyperpolarizability ($\bar{\gamma}/e^4\ a_0^4\ E_h^{-3}$) of the Dimers: Al_2P_2, Al_2As_2, Ga_2P_2, Ga_2As_2, In_2P_2, and In_2As_2 at the HF Level of Theory

		basis set description	$\bar{\alpha}$	$\Delta\alpha$	$\bar{\gamma}\times 10^3$	% increase of $\bar{\gamma}$
Al_2P_2	aug-cc-pVDZ	[6s 5p 3d/5s 4p 2d]	148.24	104.83	132	
	aug-cc-pVTZ	[6s 5p 3d 2f/6s 5p 3d 2f]	148.40	102.19	144	(+9.1)
	aug-cc-pVQZ	[7s 6p 4d 3f 2g/7s 6p 4d 3f 2g]	148.50	102.20	146	(+1.4)
Al_2As_2	aug-cc-pVDZ	[6s 5p 3d/ 6s 5p 3d]	162.50	113.35	154	
	aug-cc-pVTZ	[6s 5p 3d 2f/7s 6p 4d 2f]	162.63	110.20	167	(+8.4)
	aug-cc-pVQZ	[7s 6p 4d 3f 2g/8s 7p 6d 3f 2g]	162.59	109.92	169	(+1.2)
	aug-cc-pVDZ-PP	[6s 5p 3d/ECP10MDF + 5s 4p 3d]	163.26	114.98	158	
	aug-cc-pVTZ-PP	[6s 5p 3d 2f/ECP10MDF + 6s 5p 4d 2f]	163.25	112.19	170	(+7.6)
	aug-cc-pVQZ-PP	[7s 6p 4d 3f 2g/ECP10MDF + 7s 6p 5d 3f 2g]	163.19	111.88	171	(+0.6)
Ga_2P_2	aug-cc-pVDZ	[6s 5p 3d/5s 4p 2d]	140.69	109.96	111	
	aug-cc-pVTZ	[7s 6p 4d 2f/6s 5p 3d 2f]	141.46	108.44	119	(+7.2)
	aug-cc-pVQZ	[8s 7p 4d 3f 2g/7s 6p 4d 3f 2g]	141.55	108.51	122	(+2.5)
	aug-cc-pVDZ-PP	[ECP10MDF +5s 4p 3d/5s 4p 2d]	138.76	109.76	107	
	aug-cc-pVTZ-PP	[ECP10MDF +6s 5p 4d 2f/6s 5p 3d 2f]	139.09	108.27	114	(+6.5)
	aug-cc-pVQZ-PP	[ECP10MDF +7s 6p 4d 3f 2g/7s 6p 4d 3f 2g]	139.18	108.18	116	(+1.8)
Ga_2As_2	aug-cc-pVDZ	[6s 5p 3d/6s 5p 3d]	156.30	119.08	129	
	aug-cc-pVTZ	[7s 6p 4d 2f /7s 6p 4d 2f]	157.13	117.10	138	(+7.0)
	aug-cc-pVQZ	[8s 7p 4d 3f 2g/8s 7p 6d 3f 2g]	157.06	116.88	141	(+2.2)
	aug-cc-pVDZ-PP	[ECP10MDF +5s 4p 3d/ECP10MDF + 5s 4p 3d]	155.21	119.91	127	
	aug-cc-pVTZ-PP	[ECP10MDF +6s 5p 4d 2f/ECP10MDF +6s 5p 4d 2f]	155.42	118.31	135	(+6.3)
	aug-cc-pVQZ-PP	[ECP10MDF +7s 6p 4d 3f 2g/ ECP10MDF +7s 6p 5d 3f 2g]	155.35	117.89	137	(+1.5)
In_2P_2	aug-cc-pVDZ-PP	[ECP28MDF + 5s 4p 3d/5s 4p 2d]	171.92	150.90	154	
	aug-cc-pVTZ-PP	[ECP28MDF + 6s 5p 3d 2f/6s 5p 3d 2f]	172.37	149.35	169	(+9.7)
	aug-cc-pVQZ-PP	[ECP28MDF + 7s 7p 5d 3f 2g/7s 6p 4d 3f 2g]	172.49	149.01	170	(+0.6)
In_2As_2	aug-cc-pVDZ-PP	[ECP28MDF +5s 4p 3d/ECP10MDF + 5s 4p 3d]	189.06	155.35	181	
	aug-cc-pVTZ-PP	[ECP28MDF + 6s 5p 3d/ECP10MDF + 6s 5p 4d 2f]	188.75	157.53	196	(+8.3)
	aug-cc-pVQZ-PP	[ECP28MDF +7s 7p 5d 3f 2g/ ECP10MDF +7s 6p 5d 3f 2g]	188.98	154.59	198	(+1.0)

TABLE 2: Basis Set Dependence of the Independent Components of the Hyperpolarizability Tensor $\gamma_{\alpha\beta\gamma\delta}$ ($e^4\ a_0^4\ E_h^{-3}$) of Al_2P_2 and Ga_2As_2, at the HF Level of Theory[d]

		γ_{xxxx}	γ_{yyyy}	γ_{zzzz}	γ_{xxyy}	γ_{yyzz}	γ_{zzxx}	$\bar{\gamma}\times 10^3$
Al_2P_2	aug-cc-pVDZ	47.4	36.4	362.2	13.0	46.2	50.0	132.9
	aug-cc-pVTZ	58.3	43.5	374.7	16.1	49.3	56.3	144.0
	aug-cc-pVQZ	63.6	46.2	371.1	17.4	49.1	57.8	145.8
	aug-cc-pV5Z[a]	63.7	46.2	371.8	17.4	49.0	57.7	146.0
Ga_2As_2	aug-cc-pVDZ	43.5	41.2	349.1	12.6	43.3	49.1	128.7
	aug-cc-pVTZ	54.6	47.3	360.7	15.5	44.9	54.4	138.5
	aug-cc-pVQZ	58.1	50.8	360.2	16.5	45.6	55.6	140.9
	aug-cc-pV5Z[b]	58.7	51.2	359.6	16.7	45.5	55.6	141.0
Ga_2As_2	aug-cc-pVDZ-PP	45.2	43.6	338.0	13.4	42.8	48.3	127.1
	aug-cc-pVTZ-PP	53.8	49.5	347.3	15.7	44.4	52.4	135.1
	aug-cc-pVQZ-PP	57.2	52.3	347.4	16.6	44.6	53.3	137.2
	aug-cc-pV5Z-PP[c]	58.2	52.6	346.9	16.8	44.5	53.4	137.4

[a] Al: [8s 7p 5d 4f 3g 2h]. P: [7s 6p 5d 4f 3g 2h]. [b] Ga, As: [ECP10MDF+9s 8p 6d 4f 3g 2h]. [c] Ga, As: [ECP10MDF+8s 7p 6d 4f 3g 2h]. [d] The clusters are placed on the yz plane with the Al and Ga atoms on the z axis. All values are divided by 10^3.

electrons that each basis set provides or by the treatment of the relativistic effects that the electron core potential (ECP) of the PP basis sets furnishes. However, it would be very reasonable for one to allege that the observed differences could be related to the latter effect provided that the finite basis sets used predict properties close to the HF limit. Without a significant risk this can be claimed for the dipole polarizabilities of the clusters since it is very well-known (and our results verify it) that they converge faster than the second hyperpolarizabilities with the basis set size. Hence, judging from the predicted dipole polarizabilities of Ga_2P_2 and Al_2As_2, there are strong indications that for the III−IV cluster family, the relativistic core on the electropositive Ga atoms provides negative contributions toward the dipole polarizabilities whereas the analogue effects from the electronegative As atoms give a positive contribution. The same trend seems to be established for the second hyperpolarizabilities. Interestingly, for Ga_2As_2 the PP basis sets predict

systematically lower (hyper)polarizability values than their all electron analogues and this could be related to the stronger effect of the PP core of gallium than that of As. Indeed, the HF level polarizability calculation employed with the all electron aug-cc-pVQZ for Ga and the PP version for As yields slightly larger (hyper)polarizability values ($\bar{\alpha} \equiv 158.68$, $\bar{\gamma} \equiv 143 \times 10^3$) than the all electron basis set. On the other hand, calculations performed with the all electron aug-cc-pVQZ basis set for As and the PP set for Ga yield considerably smaller values ($\bar{\alpha} \equiv 154.73$, $\bar{\gamma} \equiv 134 \times 10^3$) than those obtained by using the all electron set.

Electron Correlation Effects. Table 3 provides a comparison between the (hyper)polarizabilities of Al_2As_2 and Ga_2P_2 calculated at the post HF levels of theory we considered in this study using the all electron aug-cc-pVDZ and PP atomic basis sets for As and Ga combined with the all electron aug-cc-pVDZ for Al and P. A careful analysis of the obtained (hyper)polarizability values reveals that the trends that are observed at the HF level hold for all correlated methods. More specifically, for Al_2As_2 all the post-HF methods yield larger (hyper)polarizabilities when a PP basis set is used. As has been observed at the HF level the observed differences are not larger than 0.6% for the mean polarizabilities of Al_2As_2 while for the mean second hyperpolarizabilities they amount to less than 2.2% differences. Also, in accord with the HF results for Ga_2P_2 the predicted (hyper)polarizabilities using the PP approach are smaller than the ones predicted with all electron basis sets and observed differences are somewhat larger than in the case of Al_2As_2 (about 1.2% for the mean polarizability and less than 3.5% for the second hyperpolarizability).

Table 4 lists the (hyper)polarizabilities of all dimers at the HF, MP2, MP4, CCSD, and CCSD(T) levels of theory. An evaluation for the predictive capability of the aug-cc-pVDZ basis set at the post HF levels of theory employed in this study, especially for the second hyperpolarizability, has been carried

TABLE 3: Electron Correlation Effects on the Mean Dipole Polarizability ($\bar{\alpha}/e^2\,a_0^2\,E_h^{-1}$), the Polarizability Anisotropy ($\Delta\alpha/e^2\,a_0^2\,E_h^{-1}$), and the Mean Dipole Hyperpolarizability ($\bar{\gamma}/e^4\,a_0^4\,E_h^{-3}$) of Al_2As_2 and Ga_2P_2 with All Electron and Pseudopotential Basis Sets[a]

			$\bar{\alpha}$	$\Delta\alpha$	$\bar{\gamma}\times10^3$				$\bar{\alpha}$	$\Delta\alpha$	$\bar{\gamma}\times10^3$
Al_2As_2	Al: [6s5p3d]	MP2	167.04	131.66	205	Al_2As_2	Al:[6s5p3d]	MP2	167.96	133.70	210
	As: [6s5p3d]	MP4	165.10	130.14	194		As: ECP+[5s4p3d]	MP4	166.00	131.95	198
		CCSD	161.75	123.49	165			CCSD	162.57	125.16	169
		CCSD(T)	163.61	127.53	180			CCSD(T)	164.46	129.21	183
Ga_2P_2	Ga: [6s5p3d]	MP2	145.06	125.95	144	Ga_2P_2	Ga: ECP+[5s4p3d]	MP2	143.14	125.44	139
	P: [5s4p2d]	MP4	143.93	126.26	139		P: [5s4p2d]	MP4	142.23	126.01	134
		CCSD	141.34	120.91	120			CCSD	139.72	120.68	117
		CCSD(T)	142.89	124.20	130			CCSD(T)	141.24	123.95	126

[a] All hyperpolarizability values are divided by 10^3.

TABLE 4: Electron Correlation Effects on the Mean Dipole Polarizability ($\bar{\alpha}/e^2\,a_0^2\,E_h^{-1}$), the Polarizability Anisotropy ($\Delta\alpha/e^2\,a_0^2\,E_h^{-1}$), and the Mean Dipole Hyperpolarizability ($\bar{\gamma}/e^4\,a_0^4\,E_h^{-3}$) of Al_2As_2 and Ga_2P_2 with the aug-cc-pVDZ Basis Set (Electron and Pseudopotential Basis Sets)[a]

		α_{xx}	α_{yy}	α_{zz}	$\bar{\alpha}$	$\Delta\alpha$	γ_{xxxx}	γ_{yyyy}	γ_{zzzz}	γ_{xxyy}	γ_{yyzz}	γ_{zzxx}	$\bar{\gamma}\times10^3$
Al_2P_2	HF	105.59	121.63	217.51	148.24	104.83	47	36	359	13	46	50	132
aug-cc-pVDZ	MP2	103.87	121.25	233.84	152.99	122.21	55	51	470	16	63	66	173
	MP4	101.59	120.19	231.16	150.98	121.34	53	49	445	15	59	63	165
	CCSD	100.65	119.19	223.74	147.86	114.95	48	43	378	14	51	54	141
	CCSD(T)	101.06	119.76	228.42	149.75	119.12	51	47	411	15	56	59	153
Al_2As_2	HF	112.32	138.65	236.52	162.50	113.35	54	44	419	15	52	59	154
aug-cc-pVDZ	MP2	110.72	136.90	253.51	167.04	131.66	63	64	557	18	73	80	205
	MP4	108.48	136.47	250.34	165.10	130.14	61	61	524	18	69	76	194
	CCSD	107.38	135.38	242.47	161.75	123.49	55	54	442	16	58	64	165
	CCSD(T)	107.85	135.91	247.08	163.61	127.53	58	58	480	17	64	71	180
Ga_2P_2	HF	94.29	114.73	213.04	140.69	109.96	37	32	300	10	39	43	111
aug-cc-pVDZ	MP2	92.54	114.58	228.06	145.06	125.95	43	48	381	13	55	56	144
	MP4	90.76	114.01	227.03	143.93	126.26	42	47	364	13	53	55	139
	CCSD	90.08	113.10	220.85	141.34	120.91	38	41	313	11	46	47	120
	CCSD(T)	90.41	113.67	224.60	142.89	124.20	41	45	337	12	51	51	130
Ga_2As_2	HF	99.49	133.42	232.71	155.21	119.91	45	44	335	13	43	48	127
aug-cc-pVDZ-PP	MP2	97.56	131.51	249.10	159.39	137.74	51	67	434	17	64	65	169
	MP4	96.06	131.95	248.01	158.67	137.56	50	65	413	16	62	63	162
	CCSD	95.44	130.96	241.31	155.90	131.75	46	57	354	15	53	54	140
	CCSD(T)	95.74	131.48	245.01	157.41	134.99	48	62	379	16	58	59	151
In_2P_2	HF	111.59	132.36	271.80	171.92	150.90	49	47	415	14	59	56	154
aug-cc-pVDZ-PP	MP2	108.89	132.8	297.46	179.72	177.82	55	73	495	18	88	74	197
	MP4	107.01	132.24	299.31	179.52	181.01	54	73	476	18	89	74	193
	CCSD	106.35	130.98	289.55	175.62	172.21	50	64	410	16	78	65	168
	CCSD(T)	106.78	131.88	296.50	178.39	178.50	52	70	433	18	86	70	181
In_2As_2	HF	120.47	153.79	291.99	188.75	157.53	62	57	489	18	63	67	181
aug-cc-pVDZ-PP	MP2	117.27	151.25	317.68	195.40	185.77	68	91	611	22	95	89	237
	MP4	115.53	151.95	318.41	195.30	187.34	67	89	584	22	95	88	230
	CCSD	114.84	150.66	308.23	191.24	178.20	62	77	498	20	81	76	198
	CCSD(T)	115.23	151.49	314.64	193.79	183.98	65	85	531	22	90	83	214

[a] All hyperpolarizability values are divided by 10^3.

out earlier for Al_2P_2[28,29] and Ga_2As_2.[25,26] For instance, for Al_2P_2 it has been shown that at MP2 and CCSD(T) levels of theory the aug-cc-pVDZ $\equiv$ [6s5p3d/5s4p2d] basis set yields (hyper)-polarizability values that are very close to those obtained with a larger optimized for this purpose [5s4p3d2f/5s4p3d2f] basis set applied in this study.[28]

Figure 2 summarizes the overall dependence of the mean (hyper)polarizabilities and the polarizability anisotropies predicted using the post-HF methods with respect to the SCF approximation. The less sensitive property to the electron correlation effects is the mean dipole polarizability whereas the mean dipole hyperpolarizabilities are considerably more sensitive. The apparent relative insensitivity of the mean polarizabilities of all dimers is caused by the different extent of the electron correlation effects on each component of the polarizability tensor. The strong electron correlation effect on each polarizability component reflects on the polarizability anisotropies which also appear to be significantly sensitive to the method

used. As shown in Figure 3a, for Al_2P_2 and In_2As_2 which provide a representative picture of all studied dimers, all post HF methods yield negative electron corrections for the perpendicular and parallel P–P and As–As bonds, components (α_{xx} and α_{yy}, respectively) whereas the electron correlation effect for the α_{zz} component (across the long diagonal) is large and positive ranging from 6% to 8% at the CCSD(T) level. Lastly, worth mentioning is the overestimation of both the longitudinal α_{zz} and α_{xx} components at the MP2 level, with respect to the CCSD(T) approximation.

For the second hyperpolarizability the CCSD(T) computations, employed with the aug-cc-pVDZ basis set, predict that the electron correlation corrected mean hyperpolarizability values for all ground state dimers lie between 15% and 20% above the corresponding SCF values. Again, notable is the overestimation of the dynamic electron correlation effect as predicted by the MP2 method. Among the principal hyperpolarizability components the largest corrections are obtained for
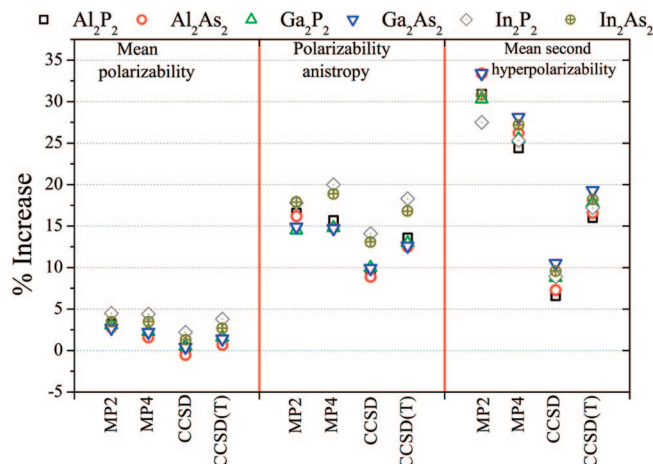
Figure 2. Post-HF increase of the mean dipole (hyper)polarizabilities and polarizability anisotropy of all studied dimers at MP2, MP4, CCSD, and CCSD(T) levels of theory employed with the aug-cc-pVDZ basis set.
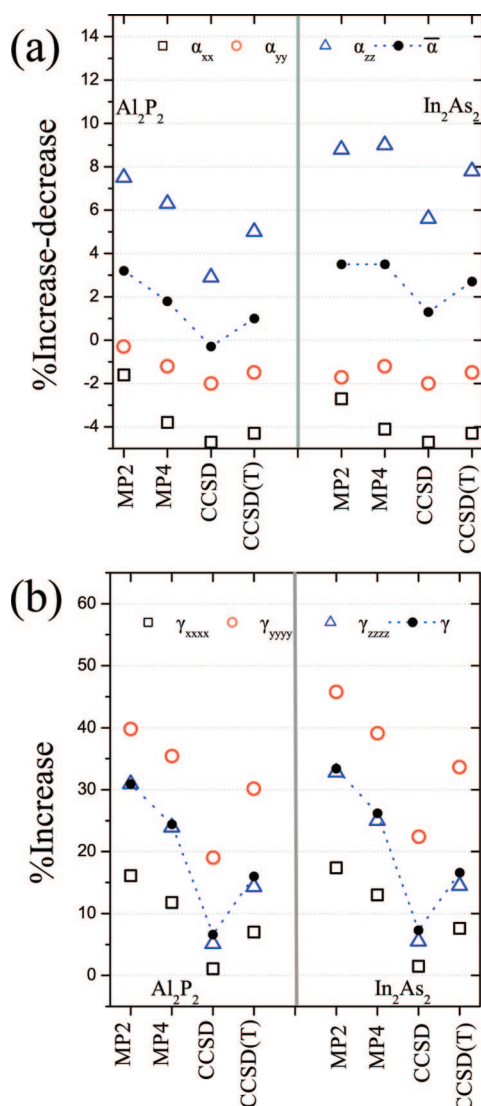

Figure 3. Increase of the axial components of the polarizability (a) and hyperpolarizability (b) tensors of Al_2P_2 and In_2As_2 dimers at MP2, MP4, CCSD, and CCSD(T) levels of theory employed with the aug-cc-pVDZ basis set with respect to the HF predicted values.

Figure 4. Comparison of the mean dipole (hyper)polarizabilities of M_2X_2 (M = Al, Ga, In and X = P, As) at HF, MP2, MP4, CCSD, and CCSD(T) levels of theory with the aug-cc-pVDZ basis set.

the γ_{yyyy} which at the CCSD(T) level are 30% to 48% larger than the corresponding SCF values (Figure 3b).[48] On the other hand, the obtained correction for the longitudinal γ_{zzzz} component is considerably smaller. Interestingly, by comparing the six independent hyperpolarizability components of Al_2P_2 and In_2As_2 it is revealed that the differences between the MP4-SDTQ and CCSD(T) values are caused mainly by the γ_{zzzz} component while the others are in relative good agreement. This shows that in all cases the interplay among the mean hyperpolarizability values calculated at the different levels of electron correlation is dominated by the predicted longitudinal γ_{zzzz} component. Accordingly, the correction obtained for the mean hyperpolarizability follows the corresponding correction for the longitudinal γ_{zzzz} at all employed levels of theory. Lastly, it should be stressed that the absolute values of the observed electron correlation corrections also depend on the basis set used. However, relying on previous experience for the III−V clusters[25−29] we believe that the general trends observed with the correlation consistent aug-cc-pVDZ basis set will not change dramatically if one utilizes sets of different sizes and construction.

Property Evolution. A comparison of the mean polarizabilities and second hyperpolarizabilities of all the studied dimers at the various levels of theory employed in this study is illustrated in Figure 4, panels a and b. The most (hyper)polarizable dimer at all levels of theory is In_2As_2, while surprisingly, the one that exhibits the smallest (hyper)polarizabilities is Ga_2P_2. Interestingly, the Al_2P_2 ground state cluster is almost as hyperpolarizable as the GaAs dimer, despite the fact that Ga_2As_2 is evidently more polarizable. The trend predicted at the HF level of theory with the aug-cc-pVDZ basis set properties holds for all basis sets employed for both the mean dipole polarizabilities and the hyperpolarizabilities, All the HF, MP4, CCSD, and CCSD(T) methods employed with the aug-cc-pVDZ basis set provide a consistent order of the mean dipole (hyper)polarizabilities $\bar{\alpha}$ and $\bar{\gamma}$ of the studied dimers:

$$\bar{\alpha} \equiv In_2As_2 > In_2P_2 > Al_2As_2 > Ga_2As_2 > Al_2P_2 > Ga_2P_2$$

$$\bar{\gamma} \equiv In_2As_2 > In_2P_2 \simeq Al_2As_2 > Al_2P_2 \simeq Ga_2As_2 > Ga_2P_2$$

It is important to point out that the second order MP theory level provides the same ordering as the rest of the methods we employed only for $\bar{\alpha}$, whereas in the case of $\bar{\gamma}$ the MP2 level predicts that Al_2As_2 is slightly more hyperpolarizable than In_2P_2.
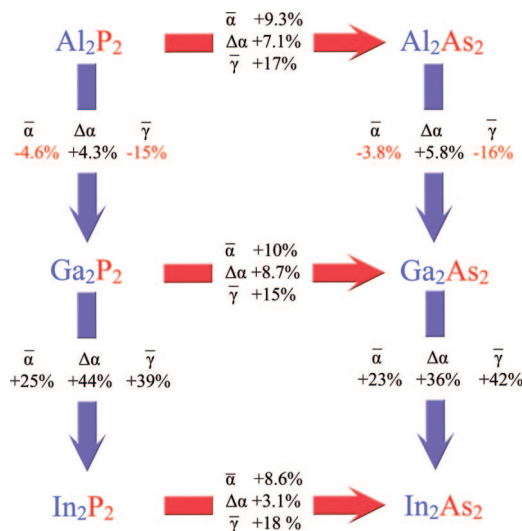
Figure 5. Schematic representation of (hyper)polarizability evolution of the M_2X_2 clusters (M = Al, Ga In, X = P, As) at the CCSD(T)/aug-cc-pVDZ level of theory.

Interestingly, regardless of the method used the observed property ordering does not match the number of electrons of each cluster. For instance, Al_2As_2 (46e) is more (hyper)polarizable than Ga_2As_2 (64e).

A schematic representation of the (hyper)polarizability evolution for the dimer ground states as one moves down to the third and the fifth row of the periodic table is presented in Figure 5. It is clear that the replacement of the phosphorus with arsenic increases consistently the (hyper)polarizabilities of the dimers. The predicted increase at the CCSD(T)/aug-cc-pVDZ level of theory for the mean polarizability amounts to $8.6-10\%$ while for the mean hyperpolarizability this increase varies between 15% and 18%. The largest increase of the polarizability anisotropy is observed on going from Ga_2P_2 to Ga_2As_2 (8.7%) and the smallest between In_2P_2 and In_2As_2 (3.1%). The obtained trend predicted for the replacement of the phosphorus with arsenic atoms correlates qualitatively with the increasing number of electrons of the clusters and with the enlargement of the size of the electronegative atom (atomic radius of P (r_P) < atomic radius of As (r_{As})).[49] Also, there is a very interesting correlation associated with the decrease of the electronegativity difference between the electropositive and the electronegative atoms of the studied clusters. More specifically, the spectroscopic electronegativity differences[50] $\Delta\chi_{spec}$ converted to Pauling scaling between [Al, Ga, In] and P are 0.640, 0.497, and 0.597 while the corresponding electronegativity differences between [Al, Ga, In] and As are 0.598, 0.455, and 0.555, respectively. In all cases the differences for the arsenic derivatives are smaller than the corresponding differences for the phosphorus clusters.

As we advance to the heavier group III elements both the polarizabilities and second hyperpolarizabilities decrease from Al to Ga, whereas their substantial increase is observed between Ga and In. The previously revealed qualitative correlation between the (hyper)polararizability increase and the increasing number of electrons of the clusters holds only for Al-In and Ga-In replacements. Also, the correlation between the decrease in the atomic electronegativity differences is valid only in the case of Al and In $(\Delta\chi_{spec}[Al-P(As)] = 0.640, (0.598); \Delta\chi_{spec}(Al-P(As)) = 0.597, (0.555)]$. The only correlation that holds throughout the entire group III is the one that involves the size of the electropositive atoms (or their atomic polarizabilities).[49] Indeed, Ga is slightly smaller than Al, and In is much larger

TABLE 5: HF and MP2 Values of the Mean Dipole Polarizability ($\bar{\alpha}/e^2\ a_0^2\ E_h^{-1}$), the Polarizability Anisotropy ($\Delta\alpha/e^2\ a_0^2\ E_h^{-1}$), and the Mean Dipole Hyperpolarizability ($\bar{\gamma}/e^4\ a_0^4\ E_h^{-3}$) of the Trimers of This Study

		$\bar{\alpha}$	$\Delta\alpha$	$\bar{\gamma}\times 10^3$
Al_3P_3-D_{3h}	HF	178.15	79.48	75
aug-cc-pVTZ	MP2	189.49	91.15	94
Al_3As_3-D_{3h}	HF	200.26	93.78	93
aug-cc-pVTZ	MP2	209.64	105.02	112
Ga_3P_3-D_{3h}	HF	172.18	79.79	72
aug-cc-pVTZ	MP2	182.19	91.36	91
Ga_3As_3-D_{3h}	HF	195.42	94.08	97
aug-cc-pVTZ	MP2	203.79	105.35	118
In_3P_3-D_{3h}	HF	211.03	101.09	110
aug-cc-pVTZ-PP	MP2	225.19	114.19	143
In_3As_3-D_{3h}	HF	236.62	114.91	141
aug-cc-pVTZ-PP	MP2	248.21	127.86	176
Al_3P_3-C_s	HF	204.31	98.95	172
aug-cc-pVTZ	MP2	212.39	113.17	225
Al_3As_3	HF	223.21	103.33	194
aug-cc-pVTZ	MP2	230.42	118.74	258
Ga_3P_3-C_s	HF	192.60	98.67	134
aug-cc-pVTZ	MP2	198.29	110.90	179
Ga_3As_3-C_s	HF	209.05	103.40	154
aug-cc-pVTZ-PP	MP2	214.10	116.40	199
In_3P_3-C_s	HF	231.28	126.96	198
aug-cc-pVTZ-PP	MP2	239.14	145.49	247
In_3As_3-C_s	HF	252.33	134.19	229
aug-cc-pVTZ-PP	MP2	259.07	152.75	287

than both Ga and Al. This points out that the reason which explains the smaller size of the Ga atoms compared to Al atoms could be related to the observed (hyper)polarizability decrease from Al to Ga. It is well-known that the atomic radius of $Ga(3d^{10}s^24p^1)$ is slightly smaller than the $Al(3s^2p^1)$ atomic radius, despite its larger number of electrons. This is caused by the insufficient shielding that the $3d^{10}$ electrons provide to the $4s^2p^1$ valence electrons of Ga. As a result of this the valence electrons of Ga experience a larger attraction from the nuclear charge than the electrons of Al. Considering that the (hyper)-polarizabilities are valence related properties and as has been demonstrated in the case of Al_nP_n[28] are affected by the electrons of the electropositive Al atoms, the described peculiarity of the Ga atoms can explain qualitatively the smaller (hyper)polariz-abilities of both Ga_2P_2 and Ga_2As_2 compared to Al_2P_2 and Al_2As_2 clusters.

Table 5 summarizes the computed (hyper)polarizabilities of the trimers considered in this work at the HF and MP2 level of theory employed with the aug-cc-pVTZ basis set. Figure 6 displays the structural data optimized at the MP2/cc-pVTZ level of theory for the two different configurations that represent the trimers. At this level, both the D_{3h} and C_s configuration correspond to true minima characterized by all real harmonic vibrational frequencies.[51,52] Figure 7a sums up the relative magnitudes of the mean dipole (hyper)polarizabilities of all studied species. As expected, the trimers are more polarizable than their corresponding dimers. Also, the C_s configurations exhibit larger polarizabilities than their planar isomers of D_{3h}
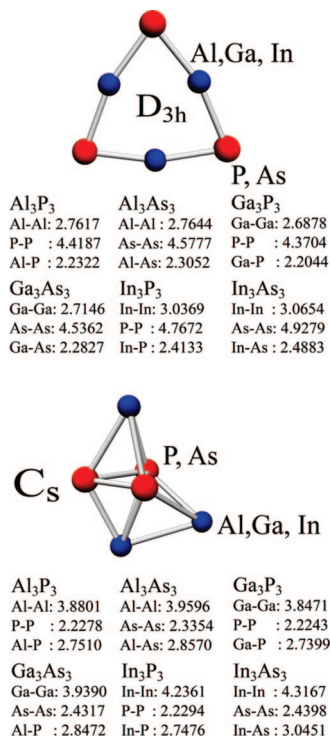
Electric Dipole (Hyper)polarizabilities

J. Phys. Chem. A, Vol. 112, No. 51, 2008 **13669**

Figure 6. MP2/cc-pVTZ optimized average bond lengths of M_3X_3 clusters (M = Al, Ga In, X = P, As).

Figure 7. (a, b) Comparison of the mean dipole (hyper)polarizabilities of M_2X_2 M_3X_3-D_{3h} and M_3X_3-C_s (M = Al, Ga, In and X = P, As) at the HF/aug-cc-pVTZ level of theory. (c) Schematic representation of the natural atomic charge evolution computed at the MP2(full)/aug-cc-pVDZ level of theory.

symmetry. This picture changes dramatically for the mean second hyperpolarizabilities. In this case the less hyperpolarizable species are the planar D_{3h} clusters. This is in perfect agreement with a recent study by Karamanis and Leszczynski[28] on the (hyper)polarizabilities of selected AlP clusters of different bonding and shapes. According to that study, Al_nP_n clusters which are characterized by large charge transfer[53] from the electropositive Al atom to the electronegative P exhibit significantly smaller hyperpolarizabilities than clusters in which the charge transfer is smaller. Our present results reveal that this trend holds for all the clusters since as it is shown in Figure 7c that the charge transfer that is estimated by the natural atomic charges on each atom of the studied clusters is larger in the case of the D_{3h} trimers than for their C_s isomers and their dimer counterparts.

The predicted trends for both the polarizability and hyperpolarizability in the case of the trimers of C_s symmetry are identical with the tendencies observed for the dimers. This can be associated to a similar bonding pattern that characterizes both the D_{2h} and C_s clusters. For instance, for Al_3As_3-C_s the atomic electron configurations of the three $Al(3s^2p^1)$ atoms are $Al(1)[core]3s^{1.83}3p^{0.66}$, $Al(2)[core]3s^{1.58}3p^{0.99}$, and $Al(3)[core]$-$3s^{1.78}3p^{0.80}$ (for the $As(4s^{24}p^3)$ atoms the electronic configurations are as follow: $As(1)[core]4s^{1.77}4p^{3.35}$ and $As(2,3)[core]$-$4s^{1.75}4p^{3.51}$). A similar picture holds for Al_2As_2 in which the 3s orbitals of the two Al atoms show comparable populations $(Al[core]3s^{1.83}3p^{0.65})$ with the Al atoms of Al_3As_3-C_s. On the other hand, in the case of Al_3As_3 the atomic natural electron configuration of the three $Al(3s^2p^1)$ in the cluster is $[core]3s^{0.91}3p^{0.23}$ while the natural electron configuration of $As(4s^2p^3)$ is represented by $[core]3s^{1.71}3p^{3.93}$. It is evident that the population of the valence 3s orbitals of Al in the case of the C_s isomers is smaller than that in the case of its D_{3h} counterpart.
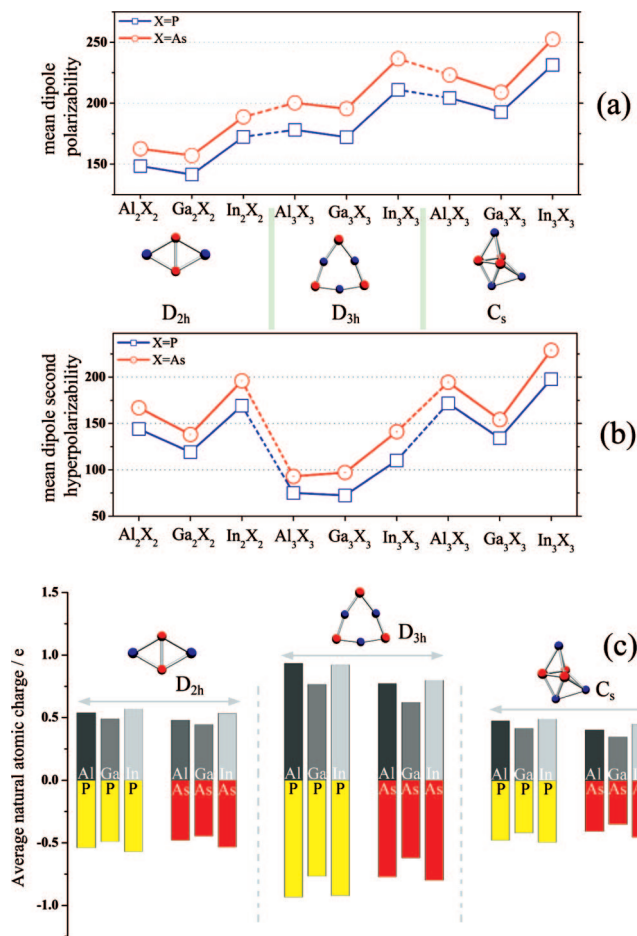
Conclusions

We have performed a systematic ab initio comparative investigation on the (hyper)polarizabilities of selected III−V semiconductor clusters. For the MP2/cc-pVTZ level optimized ground state structures of the dimer species our best HF results for the mean dipole polarizability, the polarizability anisotropy, and the mean second hyperpolarizability obtained with the aug-cc-pVQZ basis set are as follows:

$$\alpha(e^2 \, a_0^2 \, E_h^{-1}): \ Al_2P_2 \equiv 148.50, \ Al_2As_2 \equiv 163.19, \ Ga_2P_2 \equiv 139.18,$$
$$Ga_2As_2 \equiv 155.35, \ In_2P_2 \equiv 172.49, \ In_2As_2 \equiv 188.98$$

$$\Delta\alpha \, (e^2 \, a_0^2 \, E_h^{-1}): \ Al_2P_2 \equiv 102.20, \ Al_2As_2 \equiv 111.88, \ Ga_2P_2 \equiv 108.18,$$
$$Ga_2As_2 \equiv 117.89, In_2P_2 \equiv 149.01, \ In_2As_2 \equiv 154.59$$

$$\bar\gamma \, (e^4 \, a_0^4 \, E_h^{-3}): \ Al_2P_2 \equiv 146 \times 10^3, Al_2As_2 \equiv 171 \times 10^3,$$
$$Ga_2P_2 \equiv 116 \times 10^3, Ga_2As_2 \equiv 137 \times 10^3, In_2P_2 \equiv 170 \times 10^3,$$
$$In_2As_2 \equiv 198 \times 10^3$$

These values provide estimations of the (hyper)polarizabilities near the HF limit. Electron correlation is very important for the hyperpolarizabilities of those species since CCSD(T) calculations with the aug-cc-pVDZ basis set predict that the hyperpolarizabilities are at least 15−20% larger than those predicted at the HF level. The analysis of the magnitudes of the hyperpolarizabilities reveals that they are governed by the

type of electropositive atom. All methods used predict that the most hyperpolarizable clusters are the indium derivatives whereas the less (hyper)polarizable species are composed by gallium. Also, our results demonstrate how the bonding characteristics of all the investigated clusters play a vital role in their relative hyperpolarizabilities. Accordingly, clusters that are characterized by significant electron transfer from the electropositive atoms to the electronegative ones are less hyperpolarizable than species in which the electron transfer is smaller.

References and Notes

(1) *The physics of low dimensional Semiconductors*; Cambridge University Press: Cambridge, UK, 1998.

(2) (a) de Heer, W. A. *Rev. Mod. Phys. B* **1998**, *65*, 611. (b) Alivisatos, A. J. *J. Phys. Chem.* **1996**, *100*, 12336. (c) Lin, S. Y.; Fleming, J. G.; Hetherington, D. L.; Smith, B. K.; Biswas, R.; Ho, K. M.; Sigalas, M. M.; Zubrzycki, W.; Kurtz, S. R.; Bur, J. *Nature* **1998**, *394*, 251. (d) Osemann, C.; Sawitowski, T. *Chem. Soc. Rev.* **1999**, *28*, 179. (e) Rodumer, E. *Chem. Soc. Rev.* **2006**, *35*, 583. (f) Jose, R.; Zhanpeisov, U. N.; Fukumura, H.; Baba, Y.; Ishikawa, M. *J. Am. Chem. Soc.* **2006**, *128*, 629.

(3) Jin, C.; Taylor, K. J.; Conceicao, J.; Smalley, R. E. *Chem. Phys. Lett.* **1990**, *175*, 17.

(4) Klenbrander, K. D.; Mandich, M. L. *J. Chem. Phys.* **1990**, *92*, 4759.

(5) Xu, C.; de Beer, E.; Arnold, W. D.; Arnold, C. C. *J. Chem. Phys.* **1994**, *101*, 5406.

(6) Taylor, R. T.; Asmis, K. R.; Xu, C.; Neumark, D. M. *Chem. Phys. Lett.* **1998**, *133*, 140.

(7) Asmis, K. R.; Taylor, R. T.; Neumark, D. M. *Chem. Phys. Lett.* **1999**, *308*, 347.

(8) Taylor, R. T.; Comez, H.; Asmis, K. R.; Neumark, D. M. *J. Chem. Phys.* **2001**, *115*, 4620.

(9) Meloni, G.; Ferguson, J. M.; Sheehan, S. M.; Gomez, H.; Neumark, D. M. *Chem. Phys. Lett.* **2004**, *392*, 90.

(10) Becker, A. *Angew. Chem., Int. Ed. Engl.* **1997**, *36*, 1390. Schnell, M.; Herwig, C.; Becker, J. A. *Z. Phys. Chem.* **2003**, *217*, 1003.

(11) Liao, W. D.; Balasubramanian, K. *J. Chem. Phys.* **1992**, *96*, 8938.

(12) Feng, Y. P.; Balasubramanian, K. *Chem. Phys. Lett.* **1997**, *264*, 449.

(13) Feng, Y. P.; Liao, Z. M.; Balasubramanian, K. *Chem. Phys. Lett.* **1998**, *296*, 283.

(14) Feng, Y. P.; Balasubramanian, K. *J. Chem. Phys. A* **1999**, *103*, 9093.

(15) Zhang, C. *J. Chem. Phys.* **2006**, *124*, 184316.

(16) Costales, A.; Pandey, R. *Chem. Phys. Lett.* **2002**, *362*, 210.

(17) Costales, A.; Kandalam, A.; Franco, R.; Pandey, R. *J. Phys. Chem. B* **2002**, *106*, 1940.

(18) Archibong, F. E.; Amant, S. A.; Goh, K.; Marynick, S. D. *J. Phys. Chem. A* **2002**, *106*, 5932.

(19) Archibong, F. E.; Marynik, S. D. *Mol. Phys.* **2003**, *101*, 2785.

(20) Gutsev, G. L.; Johnson, E.; Mochemna, M. D.; Bauschlicher, C. W., Jr. *J. Chem. Phys.* **2008**, *128*, 144707.

(21) Guo, L.-s.; Wu, H.; Jin, Z.-h. *Int. J. Mass Spectrom.* **2004**, *240*, 149.

(22) Gallagher, B. F.; Spano, C. F. *Phys. Rev. B* **1994**, *50*, 5370.

(23) Wang, Y.; Herron, N.; Mahler, W.; Suna, A. *J. Opt. Soc. Am. B* **1988**, *6*, 808.

(24) Sharma, S.; Dewhurst, K. J.; Amprosch-Draxl, C. *Phys. Rev. B* **2003**, *67*, 165332.

(25) Karamanis, P.; Bégué, D.; Pouchan, C. *J. Chem. Phys.* **2007**, *127*, 094706.

(26) Maroulis, G.; Karamanis, P.; Pouchan, C. *J. Chem. Phys.* **2007**, *126*, 154316.

(27) Karamanis, P.; Pouchan, C.; Maroulis, G. *Phys. Rev. A* **2008**, *77*, 013201.

(28) Karamanis, P.; Leszcszynski, J. *J. Chem. Phys.* **2008**, *128*, 154323.

(29) Karamanis, P.; Xenides, D.; Leszczynski, J. *Chem. Phys. Lett.* **2008**, *457*, 137.

(30) Korambath, P. P.; Karna, S. P. *J. Phys. Chem. A* **2000**, *104*, 4801.

(31) Lan, Z. Y.; W, D.; Cheng, D. W.; Wu, S. D.; Zhang, H.; Gong, J. Y. *Chem. Phys. Lett.* **2003**, *372*, 645.

(32) Maroulis, G.; Pouchan, C. *J. Phys. Chem. B* **2003**, *107*, 10683. Papadopoulos, M. G.; Reis, H.; Avramopoulos, A.; Erkoç, S.; Amirouche, L. *J. Phys. Chem B* **2005**, *209*, 18822. *Mol. Phys.* **2006**, *104,*, 2027. Sen, S.; Chakrabarti, S. *Phys. Rev. B* **2006**, *74*, 205435.

(33) Buckingham, A. D. *Adv. Chem. Phys.* **1967**, *12*, 107.

(34) McLean, A. D.; Yoshimine, M. *J. Chem. Phys.* **1967**, *47*, 1927.

(35) Maroulis, G. *J. Chem. Phys.* **1998**, *108*, 5432. *J. Chem. Phys.*, **2003**, *118*, 2673.

(36) Szabo, A.; Ostlund, N. S. *Modern Quantum Chemistry*; MacMillan: New York, 1982.

(37) Helgaker, T.; Jørgensen, P.; Olsen J. *Molecular Electronic-Structure Theory*; Wiley: Chichester, UK, 2000.

(38) Wilson, S.; *Electron Correlation in Molecules*; Clarendon: Oxford, UK, 1984.

(39) Frisch, M. J.; Trucks, G. W.; Schlegel, H. B.; Scuseria, G. E.; Robb, M. A.; Cheeseman, J. R.; Zakrzewski, V. G. Montgomery, J. A., Jr.; Stratmann, R. E.; Burant, J. C.; Dapprich, S.; Millam, J. M.; Daniels, A. D. Kudin, K. N.; Strain, M. C.; Farkas, O.; Tomasi, J.; Barone, V.; Cossi, M.; Cammi, R.; Mennucci, B.; Pomelli, C.; Adamo, C.; Clifford, S.; Ochterski, J.; Petersson, G. A.; Ayala, P. Y.; Cui, Q.; Morokuma, K.; Rega, N.; Salvador, P.; Dannenberg, J. J.; Malick, D. K.; Rabuck, A. D.; Raghavachari, K.; Foresman, J. B.; Cioslowski, J.; Ortiz, J. V.; Baboul, A. G.; Stefanov, B. B.; Liu, G.; Liashenko, A.; Piskorz, P.; Komaromi, I.; Gomperts, R.; Martin, R. L.; Fox, D. J.; Keith, T.; Al-Laham, M. A.; Peng, C. Y.; Nanayakkara, A.; Challacombe, M.; Gill, P. M. W.; Johnson, B.; Chen, W.; Wong, M. W.; Andres, J. L.; Gonzalez, C.; Head-Gordon, M.; Replogle, E. S.; Pople, J. A. *Gaussian 98*, Revision A.11.3; Gaussian, Inc.: Pittsburgh, PA, 2002.

(40) Dolg, M. *Chem. Phys. Lett.* **1998**, *250*, 75. *J. Chem. Phys.*, **1996**, *105*, 1052.

(41) Leininger, T.; Nicklass, T.; Stoll, A.; Dolg, H.; Schwerdtfeger, M. P. *J. Chem. Phys.* **1996**, *105*, 1052.

(42) Woon, D. E.; Dunning, T. H., Jr. *J. Chem. Phys.* **1993**, *98*, 1358.

(43) Wilson, A. K.; Woon, D. E.; Peterson, K. A.; Dunning, T. H., Jr. *J. Chem. Phys.* **1999**, *110*, 7667.

(44) Peterson, K. A. *J. Chem. Phys.* **2003**, *119*, 11099.

(45) Jansik, B.; Schimmelpfennig, B.; Norman, P.; Mochizuki, Y.; Luo, Y.; Ågren, H. *J. Phys. Chem. A* **2002**, *106*, 395.

(46) Cundari, T. R.; Kurtz, H. A.; Zhou, T. *J. Phys. Chem. A* **1998**, *102*, 2962.

(47) Private communication with T. Pluta. The analytic (hyper)polarizability calculations have been carried out with the DALTON suite of programs, release 2.0 (2004), htto:/www.kjemi.uio.no/software/Dalton/.

(48) Among the various MP orders, MP2 yields the largest values and this is observed for all clusters of this study. For instance, the mean dipole hyperpolarizability of Al_2P_2 at MP3 (third order MP, is 148×10^3 au), while at MP4-DQ (doubles and quantruples substitutions) and MP4-SDQ (singles doubles and quantruples substitutions) the obtained values are 142.8 $\times 10^3$ and 145.8 $\times 10^3$ au, respectively. On the other hand, after the inclusion of triple substitutions forming the complete MP4-SDTQ method the mean (hyper)polarizability rises again to 164.5×10^3 au. A similar effect is observed in the case of the two CC methods where the inclusion of the perturbational estimate of the connected triple excitations increases considerably the second hyperpolarizability with respect to the CCSD approximation, which includes all single and double excitations.

(49) This can be related also to the atomic polarizabilities of P and As since they can be expressed as well in volume units and provide a reliable estimate of the relative atomic volumes.

(50) Allen, L. C. *J. Am. Chem. Soc.* **1989**, *111*, 9003.

(51) It is important to stress that geometry optimizations and frequency calculation of the D_{3h} configurations for Ga_3As_3 and $InAs_3$ at the B3LYP level of theory yield two soft degenerated imaginary frequencies of about $40-30$ cm^{-1}. This points out that, at this level of theory, a lower symmetry (C_s or C_1) configuration should be more stable than the D_{3h} structures. Nonetheless, if one follows the distortions, implied by the observed imaginary harmonic frequencies, the resulting structures are not very far from the planar configuration, which appears as a true minimum at the MP2 level of theory. This discrepancy between DFT and MP2 methods is quite common in small clusters of relatively high symmetry and in most of the cases is caused by the ability of the method one uses during a routine geometry optimization to treat possible pseudo-Jahn−Teller effects (see ref 52 and references therein). What is more, the disagreement between MP2 and B3LYP methods extends also to the prediction of the lowest energy structures of those species. For instance, MP2/cc-pVTZ geometry optimizations yield the Al_3P_3-C_s lower in energy for the aluminum phosphide trimer. On the other hand the B3LYP approach yields the inverse relative stability (see refs 18 and 28). We have observed a similar method performance for the rest of the phosphide clusters as well. This is a very interesting theoretical problem that, however, is beyond the scope of this paper.

Electric Dipole (Hyper)polarizabilities

J. Phys. Chem. A, Vol. 112, No. 51, 2008 **13671**

(52) Karamanis, P.; Zhang-Negrerie, P. D. Y.; Pouchan, C. *Chem. Phys.* **2007**, *331*, 417.

(53) In the present case the term "charge transfer" refers to the charge (electrons) transferred from the electropositive Al, Ga, and In atoms to the electronegative P and As after the formation of each cluster. A qualitative estimation of the relative amount of this charge can be obtained for each cluster simply by comparing the natural charges of their atoms. Accordingly, large natural atomic charges (as in the case of the trimers of D_{3h} symmetry) imply strong electron charge transfer among the electronegative and electropositive atoms (for more details see ref 28). It is important to be noted that the discussed "charge transfer" is not related to the field induced charge transfer, which has been connected to the first hyperpolarizability (especially in the case of organic push pull molecules). This property is also of significant importance; however, it is not clear yet how the bonding features of a given cluster influence its magnitude. Work is in progress to indentify possible correlations between specific cluster features and the first hyperpolarizability. The considered cluster characteristics are the cluster size, the bonding, and the cluster shape.